

DOI: <https://doi.org/10.15407/rpra29.02.113>  
UDC 537.876.23

**A.V. Brovenko, P.N. Melezhik,  
A.Ye. Poyedinchuk, O.B. Senkevych, and N.P. Yashina**

O.Ya. Usikov Institute for Radiophysics and Electronics NAS of Ukraine  
12, Acad. Proskury St., Kharkiv, 61085, Ukraine  
E-mail: pn.melezhik@gmail.com

## NATURAL ELECTROMAGNETIC MODES OF A COMPOSITE OPEN STRUCTURE INVOLVING A PERFECTLY CONDUCTING STRIP GRATING, AN INHOMOGENEOUS FERRITE LAYER, AND A MONOLAYER OF GRAPHENE

---

**Subject and Purpose.** Considered are the natural modes and their correspondent eigenfrequencies of a composite structure which is nonuniform along one of the coordinates and consists of a lossy ferromagnetic layer placed in a static magnetic field. The layer involves a perfectly conducting strip grating at one of its boundaries and a graphene monolayer at the other.

**Methods and Methodology.** The above stated problem can be approached within the analytical regularization procedure developed for dual series equations. The latter concern a broad class of diffraction problems which include, in particular, the diffraction of monochromatic plane waves on strip gratings placed at the boundary of a gyromagnetic medium. The amplitudes of the electromagnetic eigenmodes can be obtained from the infinite set of homogeneous linear algebraic equations solvable within a truncation technique. The roots of the system's determinant represent complex-valued eigenfrequencies of the system under investigation. The material parameters adopted in our computations for the ferromagnetic layer correspond to such of yttrium iron garnet.

**Results.** A number of numerical programs have been developed which permit analyzing the dependences of wave field eigenfunctions and complex eigenfrequencies upon geometrical parameters of the structure (such as grating slot width and period, and thickness of the lossy layer), as well as on electrodynamic parameters of the ferromagnet and graphene characteristics, specifically the chemical potential and relaxation energy of electrons. A number of behavioral regularities have been established, as well as the effect of non-uniformity of ferrite layer parameters upon the structure's eigenfrequencies and wave field eigenfunctions.

**Conclusions.** The structure under study has been shown to be is an open oscillatory system with a set of complex-valued natural frequencies demonstrating finite points of accumulation. The real parts of these eigenfrequencies lie in a certain interval determined by characteristic frequencies of the ferrite layer, while the imaginary parts are negative, such that the correspondent natural modes show an exponential decay with time. The grating edges represent the mirrors which the natural surface oscillations are reflected from, being supported at that by the ferromagnetic medium. The results obtained in this paper can be useful for creating the elemental base for microwave devices and the devices themselves.

**Keywords:** ferrite layer, grapheme, stripe grating, analytical regularization procedure, natural oscillations, eigenfrequencies.

---

Citation: Brovenko, A.V., Melezhik, P.N., Poyedinchuk, A.Ye., Senkevych, O.B., and Yashina, N.P., 2024. Natural electromagnetic modes of a composite open structure involving a perfectly conducting strip grating, an inhomogeneous ferrite layer, and a monolayer of graphene. *Radio Phys. Radio Astron.*, **29**(2), pp. 113–126. <https://doi.org/10.15407/rpra29.02.113>

Ц и т у в а н н я: Бровенко А.В., Мележик П.М., Поєдинчук А.Ю., Сенкевич О.Б., Яшина Н.П. Власні електромагнітні коливання відкритої композитної структури, що містить електропровідну стрічкову ґратку, неоднорідний феритовий шар і графеновий моношар. *Радіофізика і радіоастрономія*. 2024. Т. 29. № 2. С. 113–126. <https://doi.org/10.15407/rpra29.02.113>

© Publisher PH "Akademperiodyka" of the NAS of Ukraine, 2024. This is an open access article under the CC BY-NC-ND license (<https://creativecommons.org/licenses/by-nc-nd/4.0/>)

© Видавець ВД «Академперіодика» НАН України, 2024. Статтю опубліковано відповідно до умов відкритого доступу за ліцензією CC BY-NC-ND (<https://creativecommons.org/licenses/by-nc-nd/4.0/>)

## Introduction

The effects accompanying resonant interaction of electromagnetic waves with such media as magnetic materials, dielectrics, ferromagnets or plasma-like materials, currently are at the center of researchers' attention [1–7]. On the one hand, this is due to the development of technologies for synthesizing new artificial materials which may possess unusual electromagnetic (EM) properties in the microwave band. On the other hand, there is a pressing need for creating both highly reflective and EM-absorbent structures with controllable scattering properties [5, 6]. As shown in [6, 7], the presence of a periodic stripe grating at the boundary of a ferromagnet gives rise to specific resonance effects associated with excitation of magnetostatic surface waves [8, 9]. Furthermore, should there exist a periodic boundary, many familiar phenomena like the non-reciprocity effect, Faraday's effect, *etc.* [10] might manifest themselves in a highly unusual manner.

Graphene is characterized by a low-dimensional structure consisting of a single atomic layer of graphite. Owing to its unusual crystalline and electronic structures, graphene manifests unique electronic and optical properties, particularly suitable for designing devices that implement the principles of ballistic electronics, spintronics, optoelectronics, nanoplasmonics – and other prospective alternatives to the traditional semiconductor electronics. Graphene, of all solids, is characterized by the highest electron mobility which is controllable. Consequently, the problem of studying, by means of mathematical modeling, the interaction of electromagnetic radiation with graphene monolayers [11–15], is highly relevant. The modeling proceeds from solution of the Maxwell equation set together with material relations for grapheme, thus underlying the design of new types of quick, electronically controllable devices for the microwave and the terahertz bands.

The present paper is aimed at developing an analytical regularization procedure for the dual series equations which appear in a wide class of problems concerning monochromatic plane wave diffraction by a strip grating located at the boundary of a gyromagnetic medium. The procedure will be used for studying natural oscillations and eigenfrequencies of the composite structure placed in a magnetostatic field and involving a non-uniform, lossy ferromag-

netic layer with a perfectly conductive strip grating at one of its boundaries. The other boundary of the ferromagnet hosts a graphene monolayer.

As noted in paper [16], understanding the behavior of eigenfrequencies of a structure in dependence on its geometric and electrodynamic parameters could be useful for the analysis of its resonant properties. In the case of the present problem, taking into account the inhomogeneity of the ferromagnetic layer along one of the coordinates could permit finding out its impact on electrodynamic characteristics of the structure proposed, which has not yet been studied sufficiently.

## 1. Boundary-value problem: Formulation and solution

Let an open structure consisting of an inhomogeneous, lossy and gyrotropic ferromagnetic layer of thick-ness  $h$  be placed in a vacuum (the dielectric constant and the magnetic permeability of the vacuum are, respectively,  $\varepsilon_0$  and  $\mu_0$ ) (Fig. 1). The structure occupies the spatial region  $-h \leq z \leq 0$ ,  $-\infty \leq x \leq \infty$ ,  $-\infty \leq y \leq \infty$ , characterized by a tensorial magnetic permeability  $\hat{\mu}(z)$ . The upper boundary  $z = 0$  of the layer hosts a strip grating of period  $l$  which is formed by infinitely thin, perfectly conductive strips of width  $l-d$  ( $d$  is the per period width of the grating slot; the strip edges are parallel to the axis  $0x$  which is perpendicular to the plane of the figure).

The lower boundary  $z = -h$  contains a graphene monolayer of surface conductivity  $\sigma_s$ . The time dependence assumed for the monochromatic electromagnetic waves is  $e^{-i\omega t}$ , hence the material equations for the ferromagnetic medium can be written as  $\vec{D} = \varepsilon_F \varepsilon_0 \vec{E}$  and  $\vec{B} = \mu_0 \hat{\mu} \vec{H}$ . The dielectric permittivity  $\varepsilon_F$  is a complex quantity. The magnetic permeability tensor  $\hat{\mu}(z)$  for a medium placed in a magnetostatic field  $\vec{H}_0$  which is parallel to the axis  $x$  is determined as follows [10]

$$\hat{\mu}(z) = \begin{pmatrix} 1 & 0 & 0 \\ 0 & \mu_1 & i\mu_a \\ 0 & -i\mu_a & \mu_1 \end{pmatrix},$$

with

$$\mu_1 = 1 - \frac{\omega_M(z) (\omega_H^2(z) + \omega_R^2 - i\omega\omega_R)}{\omega_H (\omega^2 - \omega_H^2(z) - \omega_R^2 + 2i\omega\omega_R)}$$

and  $\mu_a = 1 - \frac{\omega\omega_M(z)}{(\omega^2 - \omega_H^2(z) - \omega_R^2 + 2i\omega\omega_R)}$ . Here  $\omega = 2\pi f$ ;  $\gamma$  is the gyromagnetic ratio;  $\omega_H = \mu_0\gamma H_0$ ;  $\omega_M = \mu_0\gamma M_0$  is the frequency characterizing magnetization of the medium, and  $\omega_R = \zeta\omega_H$ , where  $\zeta$  is the damping ratio.

The surface conductivity  $\sigma_s$  of graphene is given by Kubo's formula Eq. (1) [17], being normalized against the impedance of the vacuum,  $w_0 = (\mu_0 / \varepsilon_0)^{1/2}$ ,

$$\sigma_s = 8\alpha k_B T \ln\left(2ch\left(\frac{P_x}{2k_B T}\right)\right) \frac{i}{X + iE} + \alpha\left(\frac{\pi}{2} + \arctg \xi_- - \frac{i}{2} \ln\left(\frac{\xi_+^2}{1 + \xi_-^2}\right)\right), \quad (1)$$

where

$$\xi_{\pm} = \frac{X \pm 2P_x}{2k_B T}, \text{ and } X = \omega\hbar.$$

Here  $c = 3 \cdot 10^{11}$  mm/s is the speed of light in free space;  $\hbar = 6.582119511 \cdot 10^{-16}$  eV·s is Planck's constant;  $k_B = 8.6173332623 \cdot 10^{-5}$  eV/K the Boltzmann constant;  $T = 300$  K is Kelvin's temperature;  $E \approx 10^{-4} \div 10^{-3}$  eV is the relaxation energy of charge carriers (electrons);  $P_x = 0, \pm 0.1, \pm 0.2, \dots, \pm 1.0$  eV is the chemical potential;  $e = 1.602176634 \cdot 10^{-19}$  C the electron charge, and

$$\alpha = \frac{ew_0}{4\pi\hbar} \approx \frac{1}{137}$$

is the fine-structure constant.

Consider the spectrum of natural oscillations in the structure, assuming these to be independent of the coordinate  $x$  (*i.e.*, we will analyze the case of two-dimensional oscillations). Then, the mathematical problem concerning the spectrum of *TE*-oscillations can be formulated as follows. It is necessary to determine such values of the frequency parameter  $k = \omega\sqrt{\varepsilon_0\mu_0}$  (where  $\omega = kc$  is the eigenfrequency sought for and  $c$  the speed of light in a vacuum), which would correspond to a non-trivial solution for a homogeneous set of Maxwell's equations outside the metal strips of the grating and the graphene monolayer.

Within this formulation of the spectral problem, it follows from the Maxwell equations that the proper *TE*-mode is characterized by three non-zero field components, specifically  $E_x$ ,  $H_y$ , and  $H_z$ . The magnetic field components  $H_y$  and  $H_z$  are expressible via

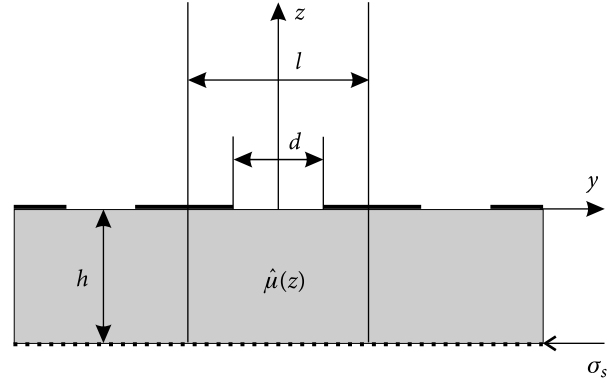


Fig. 1. Geometry of the problem

the single non-zero electric component  $E_x$  according to the formulas

$$H_y = \frac{1}{ikw_0} \times \begin{cases} \frac{\partial E_x}{\partial z}, & z > 0, \\ \frac{1}{\mu_{\perp}(z)} \left( \frac{\partial E_x}{\partial z} + i\mu_{\parallel}(z) \frac{\partial E_x}{\partial y} \right), & -h < z < 0, \\ \frac{\partial E_x}{\partial z}, & z < -h, \end{cases}$$

$$H_z = -\frac{1}{ikw_0} \times \begin{cases} \frac{\partial E_x}{\partial z}, & z > 0, \\ \frac{1}{\mu_{\perp}(z)} \left( i\mu_{\parallel}(z) \frac{\partial E_x}{\partial z} - \frac{\partial E_x}{\partial y} \right), & -h < z < 0, \\ \frac{\partial E_x}{\partial z}, & z < -h. \end{cases}$$

For the sake of brevity, we will introduce the function  $u(y, z)$  which coincides with the eigenfield's electric component  $E_x$ . As follows from the Maxwell equations, outside of the grating strips and the ferromagnetic layer-graphene boundary the function  $u(y, z)$  must satisfy

a) the Helmholtz equation,

$$\Delta u(y, z) + a(z) \frac{\partial u(y, z)}{\partial y} + b(z) \frac{\partial u(y, z)}{\partial z} + k^2 \gamma(z) u(y, z) = 0, \quad (2)$$

with

$$a(z) = \begin{cases} 0, & z > 0, \quad z < -h, \\ i\mu_{\perp}(z) \frac{d}{dz} \left( \frac{\mu_{\parallel}(z)}{\mu_{\perp}(z)} \right), & -h < z < 0, \end{cases}$$

$$b(z) = \begin{cases} 0, & z > 0, \quad z < -h, \\ -\mu_{\perp}(z) \frac{d}{dz} \left( \frac{1}{\mu_{\perp}(z)} \right), & -h < z < 0, \end{cases}$$

$$\gamma(z) = \begin{cases} 1, & z > 0, \\ \varepsilon_F(z) \mu_{\perp}(z), & -h \leq z \leq 0, \\ 1, & -h \leq z; \end{cases}$$

b) periodicity condition along the  $y$ -coordinate,

$$u(y+l, z) = u(y, z); \quad (3)$$

c) boundary conditions on the grating strips

$$u(y, z)|_{z=0+0} = 0, \quad u(y, z)|_{z=0-0} = 0; \quad (4)$$

d) field matching conditions, specifically in the grid slots, at  $z = 0$ ,

$$\begin{aligned} \frac{\partial u(y, z)}{\partial z} \Big|_{z=0+0} &= \\ &= \frac{1}{\mu_{\perp}(z)} \left( \frac{\partial u(y, z)}{\partial z} \Big|_{z=0-0} + i \mu_{\parallel}(z) \frac{\partial u(y, z)}{\partial y} \Big|_{z=0-0} \right); \end{aligned} \quad (5)$$

$$u(y, z)|_{z=0+0} = u(y, z)|_{z=0-0}; \quad (6)$$

and at the lower boundary of the graphene layer, at  $z = -h$

$$\begin{aligned} \frac{\partial u(y, z)}{\partial z} \Big|_{z=-h+0} &= \frac{1}{\mu_{\perp}(z)} \times \\ &\times \left( \frac{\partial u(y, z)}{\partial z} \Big|_{z=-h-0} + i \mu_{\parallel}(z) \frac{\partial u(y, z)}{\partial y} \Big|_{z=-h-0} \right) + \\ &+ k \sigma_s u(y, z) \Big|_{z=-h+0}; \end{aligned} \quad (7)$$

$$u(y, z)|_{z=0+0} = u(y, z)|_{z=0-0}; \quad (8)$$

e) Meixner's condition claiming that the inequality  $\iint_{\Omega} (|u|^2 + |\nabla u|^2) dy dx < \infty$  holds for any bounded and closed set  $\Omega \subset R^2$ ;

f) the radiation condition in the half-spaces  $z > 0$  and  $z < -h$ , viz.

$$u(y, z) = \begin{cases} \sum_{n=-\infty}^{\infty} R_n e^{i \frac{2\pi}{l} \Gamma_{1n} z} e^{i \frac{2\pi}{l} n y}, & z \geq 0, \\ \sum_{n=-\infty}^{\infty} T_n e^{-i \frac{2\pi}{l} \Gamma_{1n} (z+h)} e^{i \frac{2\pi}{l} n y}, & z \leq -h, \end{cases} \quad (9)$$

with  $\Gamma_{1n} = \sqrt{\kappa^2 - n^2}$  and  $\kappa = kl / 2\pi$ . The root branches  $\Gamma_{1n}$  are chosen as is shown in Fig. 2. Here  $\mu_{\perp}(z) = (\mu_1^2(z) - \mu_{\alpha}^2(z)) / \mu_1(z)$  is the effective permeability of the ferromagnetic medium magnetized to saturation, and  $\mu_{\parallel}(z) = \mu_{\alpha}(z) / \mu_1(z)$ .

Let us introduce normalized magnitudes  $\bar{y} = 2\pi y / l$ ,  $\bar{z} = 2\pi z / l$ , and  $\bar{h} = 2\pi h / l$ , and apply the separation of variables procedure to Eq. (2) (with account of the radiation condition Eq. (9)). As a result, the sought for function  $u(y, z)$  can be expressed as

$$\begin{aligned} u(y, z) &= \\ &= \begin{cases} \sum_{n=-\infty}^{\infty} R_n e^{i \frac{2\pi}{l} \Gamma_{1n} z} e^{i \frac{2\pi}{l} n y}, & z \geq 0, \\ \sum_{n=-\infty}^{\infty} (C_n^1 u_n^+(\bar{z}) + C_n^2 u_n^-(\bar{z})) e^{i \frac{2\pi}{l} n y}, & -\bar{h} < \bar{z} < 0, \\ \sum_{n=-\infty}^{\infty} T_n e^{-i \frac{2\pi}{l} \Gamma_{1n} (z+h)} e^{i \frac{2\pi}{l} n y}, & z \leq -h. \end{cases} \end{aligned} \quad (10)$$

Here  $\{R_n\}_{n=-\infty}^{\infty}$ ,  $\{C_n^1\}_{n=-\infty}^{\infty}$ ,  $\{C_n^2\}_{n=-\infty}^{\infty}$ ,  $\{T_n\}_{n=-\infty}^{\infty}$  are unknown amplitudes of the electromagnetic field components which are to be determined, and the functions  $u_n^{\pm}(\bar{z})$  are linear-independent solutions of the second-order ordinary differential equation

$$\begin{aligned} \frac{d^2 u_n^{\pm}(\bar{z})}{d\bar{z}^2} + b(\bar{z}) \frac{du_n^{\pm}(\bar{z})}{d\bar{z}} + \\ + (\kappa^2 \gamma(\bar{z}) - n^2 + ina(\bar{z})) u_n^{\pm}(\bar{z}) = 0. \end{aligned} \quad (11)$$

Using the methodology of papers [18, 19] we have obtained a homogeneous set of linear algebraic equations for determining the unknown eigenfield amplitudes,

$$\sum_{n=-\infty}^{\infty} (M_{mn} - \delta_n^m) y_n = 0, \quad m = 0, \pm 1, \pm 2, \dots \quad (12)$$

Here  $\delta_n^m$  is the Kronecker delta an

$$M_{mn} = A_{mn}(\theta, \beta) \delta_n, \quad (13)$$

$$\text{with } \theta = \frac{\pi d}{l}, \beta = \frac{1}{2\pi} \ln a, a = \frac{1 + \mu_{\perp}(0) + \mu_{\parallel}(0)}{1 + \mu_{\perp}(0) - \mu_{\parallel}(0)}.$$

The functions  $A_{mn}(\theta, \beta)$  have been found in papers [3, 4]. Next, while  $\delta_n$  equals

$$\delta_n = \Lambda_n |n| + \frac{i\mu_{\perp}(0)\sqrt{\kappa^2 - n^2} + n\mu_{\parallel}(0) - \mu_{\perp}(0)V_n(0)}{1 + \mu_{\perp}(0) - \mu_{\parallel}(0)}, \quad (14)$$

$$\text{with } \Lambda_n = \begin{cases} 1, & n \geq 0, \\ a, & n < 0. \end{cases}$$

Similar as in paper [19], it would not be difficult to demonstrate that  $C_n^1 = 0$ . The function  $V_n(z)$ , defined as

$$u_n^-(\bar{z}) = \exp\left(\int_{-\bar{h}}^{\bar{z}} V_n(\xi) d\xi\right),$$

is the solution of the Cauchy problem for the Riccati equation

$$V_n'(\bar{z}) + \mu_{\perp}(\bar{z})V_n^2 + \kappa^2 \varepsilon_F - \frac{n^2}{\mu_{\perp}(\bar{z})} - n\left(\frac{\mu_{\parallel}(\bar{z})}{\mu_{\perp}(\bar{z})}\right)' = 0, \quad (15)$$

$$V_n(-\bar{h}) = -i\left[\kappa\sigma_s + \Gamma_{1n} + in\frac{\mu_{\parallel}(-\bar{h})}{\mu_{\perp}(-\bar{h})}\right],$$

with  $V_n'(\bar{z})$  denoting the derivative of  $V_n(\bar{z})$  with respect to  $\bar{z}$ .

An approximate solution to the Cauchy problem Eq. (15) can be obtained through application of the algorithm as follows. The interval  $-\bar{h} < \bar{z} < 0$  will be specified approximately as a finite set of points  $\bar{z}_p = -\bar{h} + \delta(p-1)$ , with  $p = 1, 2, \dots, N$ ,  $\delta = \bar{h}/(N-1)$ , with  $N$  being a natural number. Recalling that  $\varepsilon_{Fp} = \varepsilon_F(\bar{z}_p)$ ,  $\mu_{\perp p} = \mu_{\perp}(\bar{z}_p)$ ,  $\mu_{\parallel p} = \mu_{\parallel}(\bar{z}_p)$  and denoting  $W_{np} = V_n(\bar{z}_p)$ , we arrive at the following recurrence relation for  $W_{np}$ ,

$$W_{np+1} = -\frac{2F_{np}}{1 + \sqrt{1 - 2\delta\mu_{\perp p+1}F_{np}}}, \quad n = 0, \pm 1, \pm 2, \dots, \quad p = 1, 2, \dots, N-1,$$

$$W_{n1} = -i\left[\kappa\sigma_s + \Gamma_{1n} + in\frac{\mu_{\parallel 1}}{\mu_{\perp 1}}\right], \quad (16)$$

where

$$F_{np} = -W_{np} + \frac{\mu_{\perp p}\delta}{2}W_{np}^2 + \frac{\kappa^2\delta}{2}(\varepsilon_{Fp} + \varepsilon_{Fp+1}) - \frac{n^2\delta}{2}\left(\frac{1}{\mu_{\perp p}} + \frac{1}{\mu_{\perp p+1}}\right) - n\left(\frac{\mu_{\parallel p+1}}{\mu_{\perp p+1}} - \frac{\mu_{\parallel p}}{\mu_{\perp p}}\right).$$

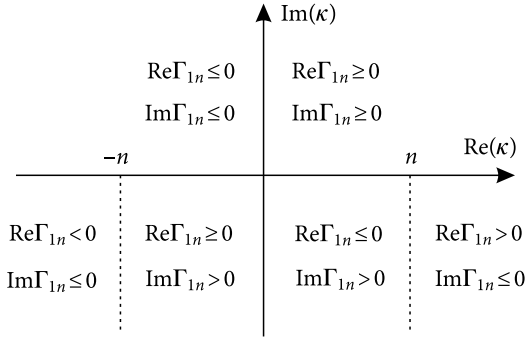


Fig. 2. Selecting branches of the root function  $\Gamma_{1n}$

The square root in Eq. (16) can be calculated as follows

$$\sqrt{1 - 2\delta\mu_{\perp p+1}F_{np}} = \left|\text{Re}\left(\sqrt{1 - 2\delta\mu_{\perp p+1}F_{np}}\right)\right| + i\text{Sign}\left(-\text{Im}\left(\mu_{\perp p+1}F_{np}\right)\right)\left|\text{Im}\left(\sqrt{1 - 2\delta\mu_{\perp p+1}F_{np}}\right)\right|.$$

The eigenfield Eq. (10) can be represented as an expansion in non-trivial solutions  $y_n$  of the equation set Eq. (12), viz.:

$$E_x(\bar{y}, \bar{z}) = \begin{cases} \sum_{n=-\infty}^{\infty} (y_n - \delta_n^0) e^{i\frac{2\pi}{l}\Gamma_{1n}\bar{z}} e^{i\frac{2\pi}{l}n\bar{y}}, & \bar{z} \geq 0, \\ \sum_{n=-\infty}^{\infty} y_n \frac{B_{nN}}{B_n(\bar{z})} e^{i\frac{2\pi}{l}n\bar{y}}, & -\bar{h} < \bar{z} < 0, \\ \sum_{n=-\infty}^{\infty} y_n B_{nN} e^{i\frac{2\pi}{l}n\bar{y}}, & \bar{z} \leq -\bar{h}, \end{cases} \quad (17)$$

where the functions  $B_{np}(z)$  are to be calculated through the use of the recurrence relation

$$B_{np+1} = B_{np} e^{-0.5\delta(\mu_{\perp p}W_{np} + \mu_{\perp p+1}W_{np+1})}, \quad B_{n1} = 1, \quad n = 0, \pm 1, \pm 2, \dots, \quad p = 1, \dots, N-1.$$

When formulating the eigenvalue problem, we proceeded from the conceptual assumption that the solution should reflect those features of the diffraction field  $(\vec{E}^d, \vec{H}^d)$  which arise during its analytical continuation into the complex frequency domain [20, 21]. The grating involving a ferromagnetic layer and a graphene insert can be represented as an open resonant structure characterized by complex-valued eigenfrequencies and their correspondent natural oscillations. The spectral parameter to be determined is represented by the frequency  $\omega(\kappa = l\omega/2\pi c)$ . The radiation condition which is characteristic of diffraction problems is continued analytically from the real

frequency region onto an infinite-sheeted Riemann surface (see [20]). We will limit ourselves by making account of the "physical" sheet of the Riemann surface for  $\Gamma_{1n} = \sqrt{\kappa^2 - n^2}$  (the choice of root branches is defined in Fig. 2).

The solution to the spectral problem considered is represented by the non-zero solution for a homogeneous set of linear algebraic equations (12). The matrix elements in Eq. (12) are considered as functions of the spectral parameter  $\kappa$  which latter exists on the "physical" sheet of the Riemann surface. As has been proven, through the use of the results of paper [21], the matrix operator  $M(\kappa) = \{M_{mn}(\kappa)\}_{m,n=-\infty}^{\infty}$  is a kernel-operator analytic function of the complex variable  $\kappa$  everywhere except the points  $\kappa = 0$ , as well as branch points  $\hat{\kappa}_n, n = 0, \pm 1, \pm 2, \dots$ . Therefore, the complex eigenfrequencies are represented by roots of the equation

$$\det(M(\kappa) - I) = 0, \tag{18}$$

where the  $\det(\dots)$  symbol means an infinite determinant of the operator  $M(\kappa) - I$ . The equation permits of an effective numerical solution. Indeed, let  $M_P(\kappa)$  be a finite-dimensional operator function obtainable through truncation of the matrix  $M(\kappa)$  toward the size  $P \times P$ . Because of the kernel property of  $M(\kappa)$ , it proves possible to guarantee the existence of  $P$ , such that

$$\|M(\kappa) - M_P(\kappa)\| < \delta, \tag{19}$$

for any arbitrarily small  $\delta > 0$  and any limited domain of variation for  $\kappa$ . (Here  $\|\dots\|$  stands for operator norm in the space  $l_2$ ). The eigenfrequencies of the finite-dimensional operator function  $I - M_P(\kappa)$  can be found as roots of the determinant  $\det(M_P(\kappa) - I)$ . Provided that Eq. (19) is satisfied, each solution  $\kappa_m$  of the spectral problem Eq. (18) can be approximated to, with any predetermined accuracy, by a solution of the  $\kappa_m^P$  finite-dimensional spectral problem for the  $M_P(\kappa) - I$  operator function with a sufficiently high  $P$ . Using the kernel property of the operator-function  $M(\kappa)$ , one can demonstrate that the procedure described is computationally stable for growing values of  $P$  [22].

In what follows below, we also need to consider excitation of the structure by a plane,  $E$ -polarized electromagnetic wave obliquely incident upon the

structure. The electric field vector of the  $E$ -polarized electromagnetic wave should be parallel to the axis  $Ox$ , and the wave vector  $\vec{k}$  should lie within the plane  $(y, z)$ , making an angle  $\alpha$  with the axis  $z$ . The non-zero field components of the wave need to be of form

$$E_x^0 = e^{ik(y \sin \alpha - z \cos \alpha) - i\omega t},$$

$$H_y^0 = -\frac{\cos \alpha}{w_0} E_x^0, \quad H_z^0 = -\frac{\sin \alpha}{w_0} E_x^0.$$

It can be shown that for the case of real frequencies ( $k = \omega \sqrt{\epsilon_0 \mu_0}$ ) the diffraction problem described has a unique solution (see [21] for details).

Following the approach of papers [3, 18, 19] (and leaving some minor details aside) we can obtain an inhomogeneous set of linear algebraic equations for determining the unknown amplitudes of the diffracted electromagnetic field,

$$\sum_{n=-\infty}^{\infty} (C_{mn} - \delta_n^m) y_n = B_m, \tag{20}$$

where

$$C_{mn} = \delta_n^v A_{mn}(\theta, \beta, \nu), \quad B_m = \frac{2i\mu_{\perp}(0)}{1 + \mu_{\perp}(0) - \mu_{\parallel}(0)} \times$$

$$\times A_{mn_0}(\theta, \beta, \nu) \sqrt{\kappa^2 - (n_0 + \nu)^2}, \quad m = 0, \pm 1, \pm 2, \dots,$$

$A_{mn}(\theta, \beta, \nu)$  are defined in [3];  $\kappa \sin \alpha = n_0 + \nu$  with  $0 \leq \nu < 1$ , and  $\delta_n^v = \Lambda_n |n + \nu| +$

$$+ \frac{i\mu_{\perp}(0) \sqrt{\kappa^2 - (n + \nu)^2} + (n + \nu) \mu_{\parallel}(0) - \mu_{\perp}(0) V_n^v(0)}{1 + \mu_{\perp}(0) - \mu_{\parallel}(0)}$$

(compare with the  $\delta_n$  of Eq. (14)). Similarly, the solutions  $V_n^v(\bar{z})$  of the Cauchy problem coincide with the functions Eq. (15) if  $n$  has been replaced by  $n + n_0 + \nu$ .

The diffracted field is given by Eq. (17), with the reflection coefficient  $R$ , the transmission ratio  $T$  and the absorption coefficient  $W$  specified, respectively, as

$$R = y_{n_0} - 1, \quad T = B_{n_0 N} \gamma_{n_0},$$

$$W = 1 - |R|^2 - |T|^2. \tag{21}$$

The method proposed has been implemented in the form of program complexes enabling calculations of spectral characteristics of the eigenfrequencies and electromagnetic eigenfields over the entire frequency range. The programs are efficient for a va-

riety of geometric and electrodynamic parameters of the structure. including the regions where the real part of the ferromagnet's effective permeability may turn negative.

## 2. Numerical results

The method developed has been used for calculating eigenfields and complex-valued eigenfrequencies in dependence on the structural parameters. The material parameters of the ferromagnetic layer (specifically, of its constituent yttrium iron garnet) are  $4\pi M = 1750$  G,  $H_0 = 750$  Oe,  $\varepsilon_F = 15.30$ , and  $\zeta = 0.01$ , while such of the graphene monolayer have been evaluated as  $P_x = 0.3$  eV,  $E = 10^{-4}$  eV, and  $T = 300$  K. (Note the magnitudes of the magnetization vector  $\vec{M}$  and the magnetic field  $H_0$  to be expressed here in the CGS rather than SI system of units). Hereinafter, all the results will be given in terms of the linear frequencies  $f = \omega / 2\pi$ . The frequency range being investigated is  $\sqrt{f_H^2 + f_H f_M} < \text{Re } f < f_H + 0.5 f_M$ , wherein the real part  $\text{Re } \mu_{\perp}$  of the effective permeability assumes negative values. The choice of this range owes partly to the fact that, according to papers [8, 9], the ferromagnet–vacuum interface can support surface spin waves as directly propagating excitations (their group and phase velocity vectors are parallel to each other). A metal strip grating placed at the interface can provide a "source" for exciting the surface spin waves. The results below seem to support these assumptions. First, we will determine resonant responses of the structure under investigation for the cases where it either does or does not involve the graphene layer — or the ferromagnetic layer, with or without the graphene. This concerns the strip lattice as well. The dependences of the power reflection coefficient  $|R|^2$  of a plane wave incident normally on some of the structures are shown in Fig. 3. Here, the grating period is  $l = 1$  mm, the slot width  $d = 0.5$  mm, and the ferromagnetic layer's thickness is  $h = 0.05$  mm. Also, Fig. 3 demonstrates the following. In case the layer contains neither grating, nor graphene, the power reflection coefficient  $|R|^2$  shows a maximum at the ferromagnetic resonance frequency [10], namely  $f \approx \sqrt{f_H^2 + f_H f_M} = 3847.2$  MHz (curve 4). Outside the vicinity of this frequency,  $|R|^2$  is almost zero, which suggests total transmission of the plane wave through the ferromagnetic layer. With the graphene monolayer placed on the

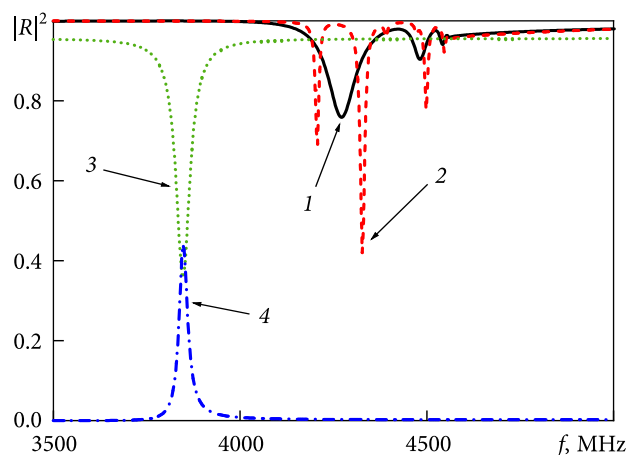
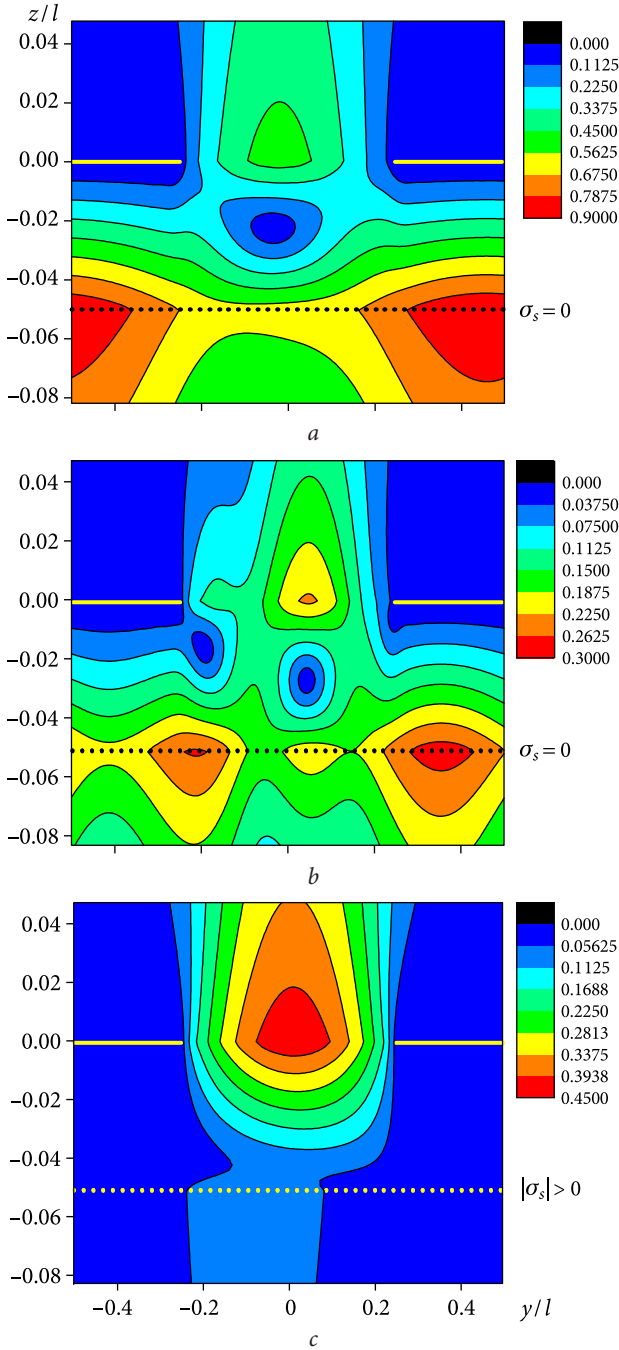


Fig. 3. Power reflection coefficient  $|R|^2$  as a function of frequency: curve 1 relates to the case of a layer containing grating and graphene; curve 2, layer with grating, no graphene; curve 3, layer with graphene, and curve 4, layer without graphene

lower boundary of the layer, the picture turns exactly opposite. The reflection coefficient  $|R|^2$  gets almost equal to one outside the vicinity of the ferromagnetic resonance, meaning total reflection of the plane wave there, whereas it is minimized at the resonance frequency itself (see curve 3).

As can be seen, a graphene monolayer present at the lower boundary of the ferromagnetic layer does significantly change resonance properties of the structures under study. In case both the grating and graphene are present, the number of resonant responses happens to be nearly twice lower than in the absence of graphene, similarly as the intensity of the response. The reason why is the presence of an "impedance-type" boundary condition at the lower border of the ferromagnetic layer, which owes to the finite conductivity of graphene. That latter excises the resonance frequencies at which the surface oscillations are excited, the field of which tends to be concentrated at the lower boundary of the layer (see Figs. 4, a and b). The spectrum contains only such resonance frequencies which correspond to the surface oscillations concentrated at the upper boundary of the ferromagnet (between the grating edges, see Fig. 4, c).

As was shown in paper [16], a planar grating with a layer of metamaterial on it can be interpreted as an open resonant structure characterized by complex-valued eigenfrequencies and their respective natural oscillations. Accordingly, the set of discrete values of the frequency parameter  $\kappa$  is close to the



**Fig. 4.** Resonant fields  $|E_x| = \text{const}$  demonstrated by a grating which involves a ferromagnetic layer without graphene. Panel (a):  $f = 4207.2$  MHz; Panel (b):  $f = 4498.2$  MHz; Panel (c): fields of frequency  $f = 4273.2$  MHz in a layer containing a grating and graphene

set of real parts of the eigenfrequencies — under the conditions where the structure provides either for resonant reflection or for resonant transmission of the field's energy.

In what follows, we will focus on analyzing the structure's eigenfrequencies (that is, solutions to the

equation  $\det(M(\kappa) - I) = 0$ ) and the natural oscillations

$$\sum_{n=-\infty}^{\infty} (M_{mn} - \delta_n^m) y_n = 0, \quad m = 0, \pm 1, \pm 2, \dots,$$

which are solutions of the equation set Eq. (12). We will also consider the eigenfield representations Eq. (17).

In the case of a ferromagnetic layer with graphene sitting at the lower boundary, the dispersion equation takes the form

$$e^{2i\kappa\sqrt{\varepsilon_F\mu_\perp}h} \left( 1 - \sqrt{\frac{\varepsilon_F}{\mu_\perp}} + (1 + \sigma_s) \left( 1 - \sqrt{\frac{\mu_\perp}{\varepsilon_F}} \right) \right) + 1 + \sqrt{\frac{\varepsilon_F}{\mu_\perp}} + (1 + \sigma_s) \left( 1 + \sqrt{\frac{\mu_\perp}{\varepsilon_F}} \right) = 0. \quad (22)$$

Upon solving this equation for the above specified parameters of the ferromagnetic layer, we obtain a complex-valued eigenfrequency of the ferromagnetic resonance as  $f_{FMR} = (3846.46 - i63.53)$  MHz. The resonance frequency for the graphene layer presented in Fig. 3 (curve 3) is  $f_{rez} = 3847.17$  MHz. Thus, the resonant excitation of the layer owes to excitation of the eigenmode corresponding to ferromagnetic resonance. The small shift of the resonance frequency from the real part of the eigenfrequency is due to the presence of an imaginary part in the eigenfrequency. The effect is characteristic of all cases of resonant excitation of natural oscillations.

With a strip grating placed at the upper boundary of the ferromagnetic layer the structure turns into kind of an open resonator for the surface oscillations. The grating edges are resonator mirrors which reflect the surface natural oscillations, while the ferromagnetic medium supports these, thus leading to appearance of resonances in the frequency dependence of the reflection coefficient  $|R|^2$  (see Fig. 3). Some examples are shown below of the dependences upon geometric and electrodynamic parameters of the structure which are demonstrated by the complex eigenfrequencies and the natural oscillations.

Having analyzed the results presented in Fig. 5, we are in a position to draw conclusions as follows. First, three complex-valued eigenfrequencies are identifiable for the structure's parameters selected. They are significantly dependent on the geometric characteristics (note that the number of eigenmodes

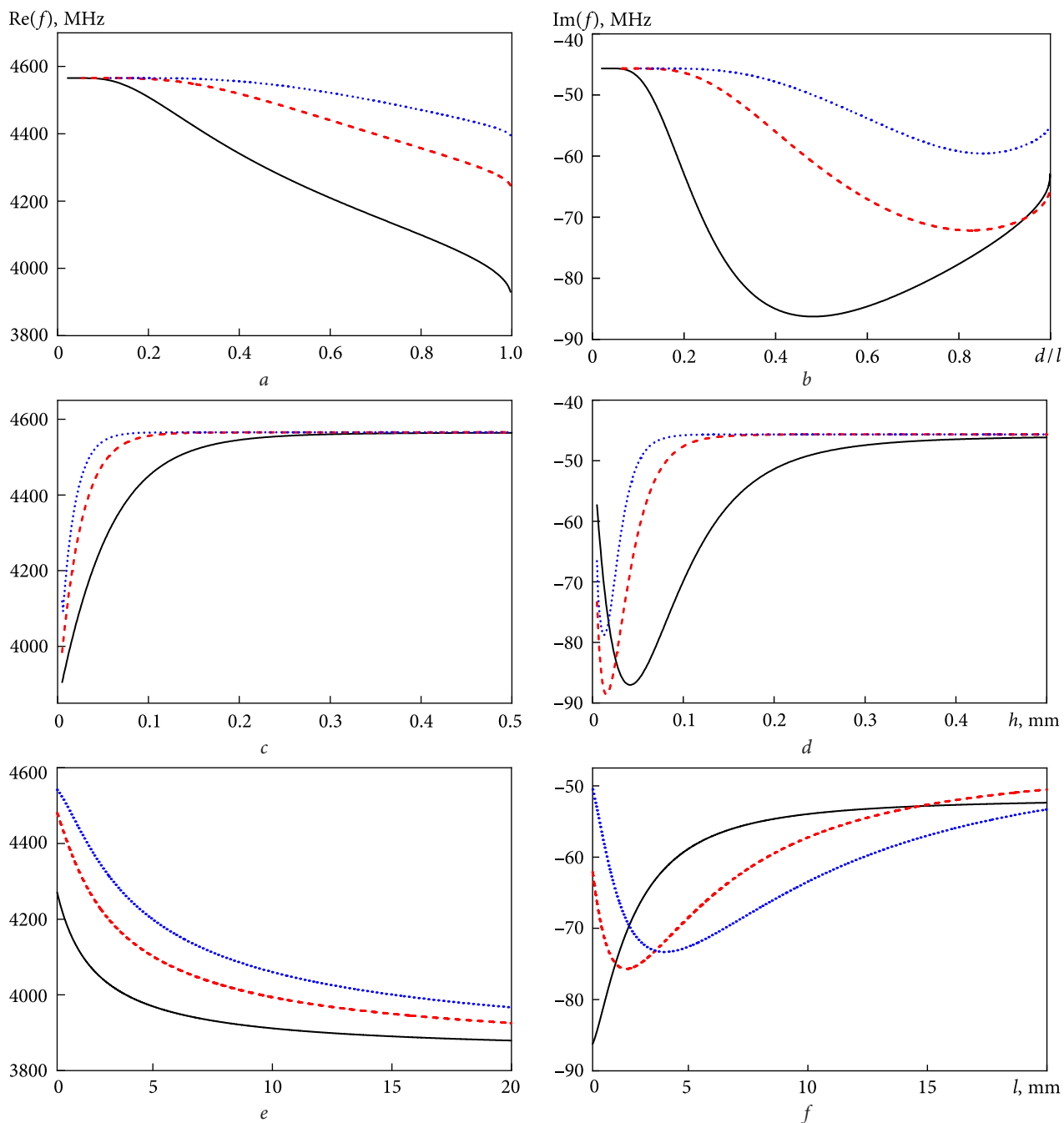


**Fig. 5.** Real and imaginary parts of the eigenfrequencies as dependent on geometrical parameters. Panel (a):  $\text{Re}(f)$ , and Panel (b):  $\text{Im}(f)$  versus the slot width normalized per grating period, for  $l = 1$  mm and  $h = 0.05$  mm; Panels (c) and (d) – same versus layer thickness, for  $l = 1$  mm and  $d = 0.5$  mm; Panels (e) and (f):  $\text{Re}(f)$  and  $\text{Im}(f)$ , respectively, versus the grating period, for  $d = 0.5$  mm and  $h = 0.05$  mm

can be either higher or lower, depending on magnitudes of other geometrical parameters). Second, by changing the geometric parameters we can obtain any value of the eigenfrequency's real part from the range  $3847.2 \text{ MHz} \approx \sqrt{f_H^2 + f_H f_M} \leq \text{Re}(f) \leq f_H + 0.5 f_M \approx 4565.6 \text{ MHz}$ , thus being able to control the resonant modes. With  $d/l \rightarrow 1$ ,  $h \rightarrow 0$ , and  $l \rightarrow \infty$

the eigenfrequencies tend to the accumulation point  $f_{\text{FMR}} = (3846.46 - i63.53) \text{ MHz}$  *i.e.*, the ferromagnetic resonance frequency. With  $d/l \rightarrow 0$ ,  $h \rightarrow 1$ , and  $l \rightarrow 0$  the eigenfrequencies tend to the accumulation point  $f = (4565.5 - i45.65) \text{ MHz}$  associated with the characteristic frequency  $f = f_H + 0.5 f_M$  of the ferromagnetic layer.

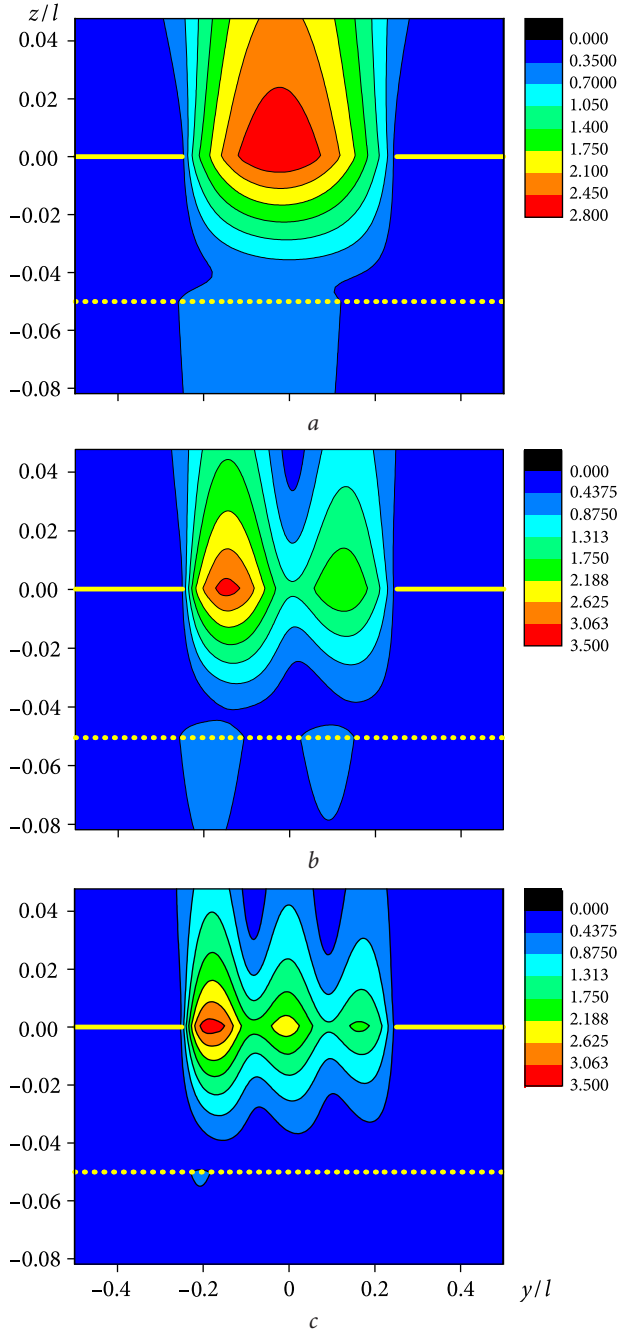


**Fig. 6.** Eigenfield distributions of  $TE_m 0$ -modes. Panel (a):  $TE_{10}$ -mode at  $f = (4270.8 - i86.2)$  MHz; Panel (b):  $TE_{20}$ -mode at  $f = (4481.3 - i62.1)$  MHz, and Panel (c):  $TE_{30}$ -mode at  $f = (4541.7 - i50.5)$  MHz. In all the cases,  $h = 0.05$  mm,  $l = 1$  mm and  $d = 0.5$  mm

Fig. 6 demonstrates the eigenfields  $|E_x| = \text{const}$  corresponding to these eigenfrequencies. As can be seen from comparison of Figs. 6, *a* and 4, *c*, the field excited at the real-valued resonance frequency is of similar structure with the natural oscillation. In addition, the structure of the eigenfields of Fig. 6 clear-

ly suggests that the strip grating is a provocateur for excitation of the higher-order surface harmonics in the proposed structure — in those cases where the surface-mode electromagnetic field involves several antinodes in between the grating edges.

Below, we will use the notation as follows. A natural oscillation will be termed the  $TE_{mn}$ -mode, should it demonstrate  $m$  crests of the  $|E_x|$  per the structures period at the upper boundary (between the grating edges) and  $n$  crests at the lower boundary.

Let us discuss the effect of graphene parameters on the eigenfrequencies. Fig. 7 and 8 demonstrate that changes in the graphene parameters do have some influence on magnitudes of the eigenfrequencies, although the resultant effect is not as significant as the changes in the geometric parameters. At the same time, by varying  $P_x$  or  $E$  it is possible to control the real part of the eigenfrequency (or, the resonance frequency of the excitation) over the 50 MHz range.

The studies of ferrite film properties have shown that the spatial inhomogeneity of their magnetic parameters can strongly influence the conditions for the excitation and propagation of surface spin waves in such systems. Inhomogeneities of either the magnetostatic field distributions [23] or saturation magnetization [24] can lead to a change in the absorption spectrum of the surface spin excitations, as well as to appearance of new absorption lines, and to changes in the attenuation of the surface spin waves. To study these phenomena, some physical models have been proposed that take into account the spatial inhomogeneity of one or more magnetic parameters [23, 24] — most often, in directions perpendicular to the plane of the ferrite film. In the simplest case, the inhomogeneity profile of any parameter was a step function with one or more split points inside the film [24].

Proceeding from the above considerations, we have resorted to a rigorous methodology for analyzing the effect of non-uniformity of the magnetostatic field,  $H_0$  and the saturation magnetization,  $M_0$ . Let the non-uniformity exist along just one of the coordinates, specifically,  $z$ , and let it be described in terms of the dimensionless, frequency-dependent parameters of the permeability tensor as

$$\kappa_M(z) = g_i(z)\kappa_M^0, \kappa_H(z) = g_i(z)\kappa_H^0,$$

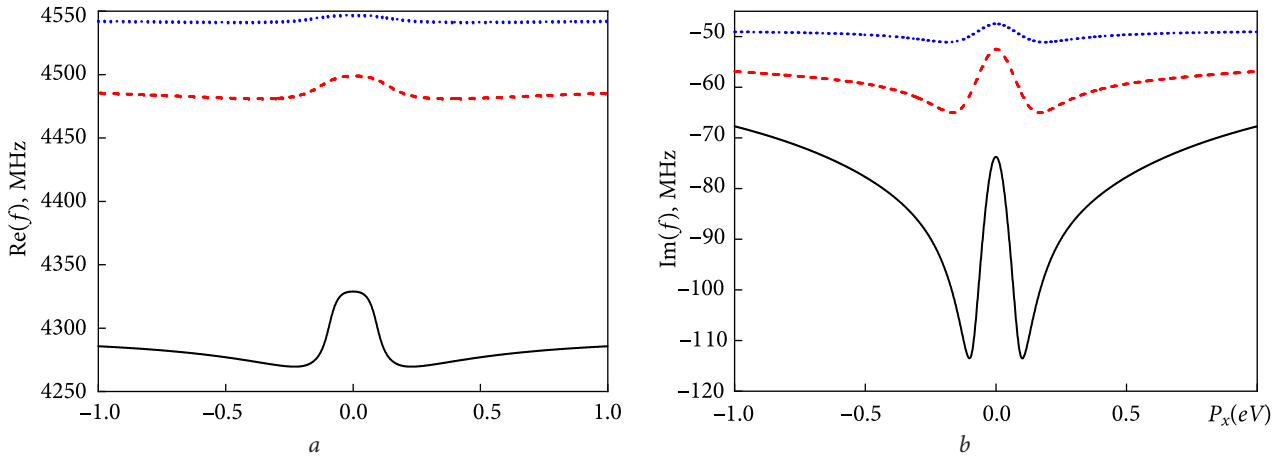


**Fig. 7.** The real, Panel (a), and imaginary, Panel (b), parts of the eigenfrequencies for modes  $TE_{m0}$  with  $m = 1, 2,$  and  $3,$  as functions of the chemical potential  $P_x$  (solid line:  $m = 1;$  dashed line:  $m = 2,$  dotted line:  $m = 3$ ), all with  $l = 1$  mm,  $d = 0.5$  mm,  $h = 0.05$  mm,  $E = 10^{-4}$  eV

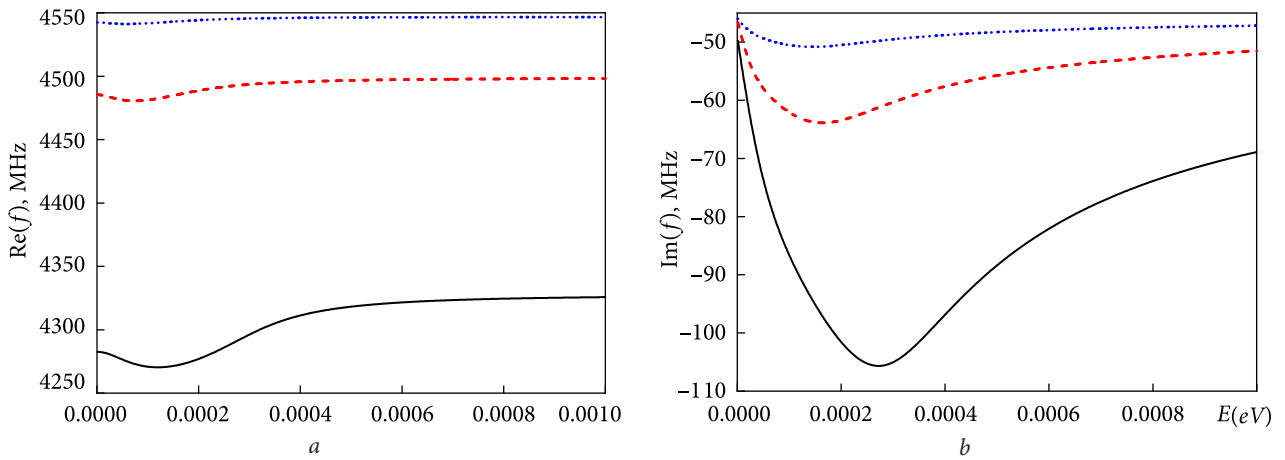


**Fig. 8.** The real, Panel (a), and imaginary, Panel (b), parts of the eigenfrequencies for modes  $TE_{m0}$  with  $m = 1, 2,$  and  $3,$  as functions of the charge carriers' relaxation energy  $E$  (solid line:  $m = 1;$  dashed line:  $m = 2,$  and dotted line:  $m = 3$ ), with  $l = 1$  mm,  $d = 0.5$  mm,  $h = 0.05$  mm,  $P_x = 0.3$  eV

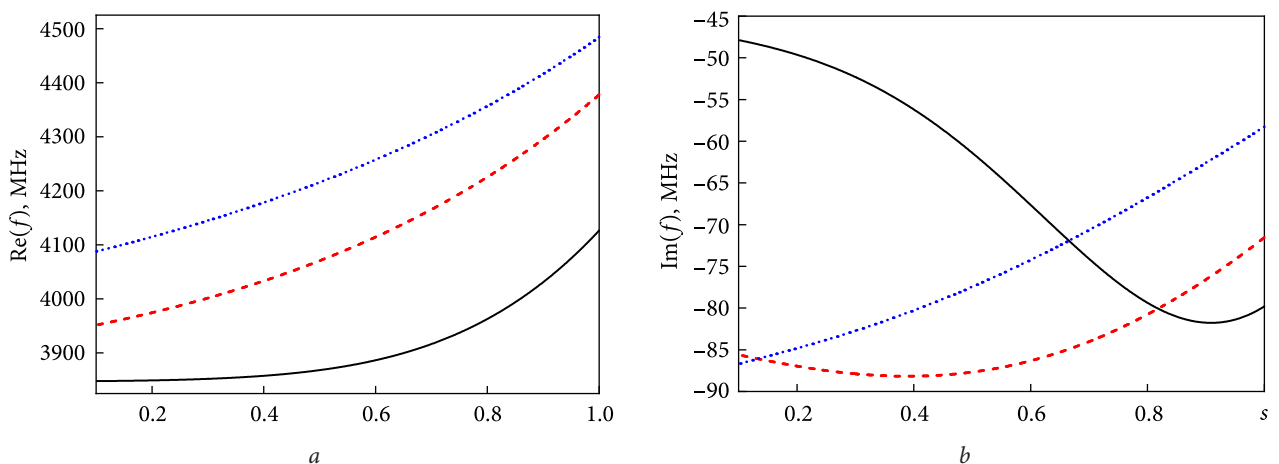


**Fig. 9.** The real, Panel (a), and imaginary, Panel (b), parts of the eigenfrequencies for modes  $TE_{m0}$  with  $m = 1, 2,$  and  $3,$  in dependence on the degree  $s$  of the magnetostatic field's inhomogeneity, with  $g_1(\bar{z}) = (1 - s)\bar{z} + 1$  (solid line:  $m = 1;$  dashed line:  $m = 2,$  and dotted line:  $m = 3$ )

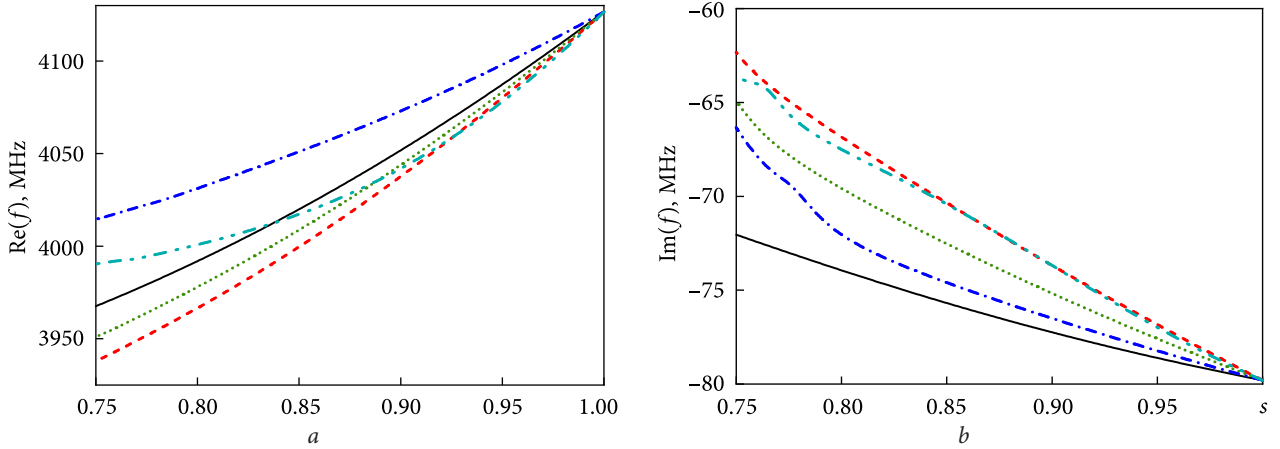


**Fig. 10.** The eigenfrequencies real (a) and imaginary (b) parts for modes versus the inhomogeneity degree  $s$  of the saturation magnetization for various functions  $g_i(\bar{z})$ ,  $i = 1$  – solid line;  $i = 2$  – dashed line;  $i = 3$  – dotted line;  $i = 4$  – dash-dotted line;  $i = 5$  – dash-dotted – dotted line

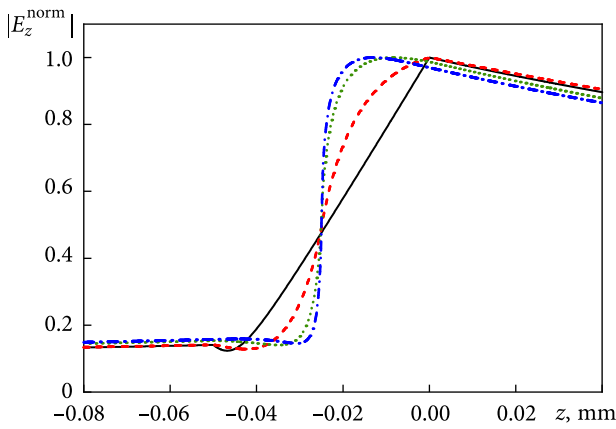


**Fig. 11.** The dependences shown by the amplitudes of the  $TE_{10}$  oscillations (normalized against their maximum value) as registered at the axis passing through the middle of the grating slot for various values of the magnetostatic field's inhomogeneity degree  $s$  (solid line:  $s = 1$ ; dashed line:  $s = 0.7$ ; dotted line:  $s = 0.365$ , and dash-dotted line:  $s = 0.101$ ), with

$$g_3(\bar{z}) = \begin{cases} (2 - 2s)\bar{z} + (2 - s), & -1 \leq \bar{z} \leq -0.5, \\ (-2 + 2s)\bar{z} + s, & -0.5 \leq \bar{z} \leq 0 \end{cases}$$

with

$$\kappa_M^0 = \frac{\gamma M_0 l}{2\pi c}, \quad \kappa_H^0 = \frac{\gamma H_0}{2\pi c}, \quad \kappa_R = \frac{\zeta \gamma H_0}{2\pi c}, \quad \text{and}$$

$$\mu_1(z) = 1 - \frac{\kappa_M(z) (\kappa_H^2(z) + \kappa_R^2 - i\kappa\kappa_R)}{\kappa_H (\kappa^2 - \kappa_H^2(z) - \kappa_R^2 + 2i\kappa\kappa_R)},$$

$$\mu_a(z) = \frac{\kappa\kappa_M(z)}{(\kappa^2 - \kappa_H^2(z) - \kappa_R^2 + 2i\kappa\kappa_R)}.$$

The functions  $g_i(z)$  that have been selected for specifying the type of the inhomogeneity type, are expressed as  $g_1(\bar{z}) = (1 - s)\bar{z} + 1$ , with  $-1 \leq \bar{z} \leq 0$ ,

and  $g_2(\bar{z}) = (s - 1)\bar{z} + s$ , with  $-1 \leq \bar{z} \leq 0$ , and also

$$g_3(\bar{z}) = \begin{cases} (2 - 2s)\bar{z} + (2 - s), & -1 \leq \bar{z} \leq -0.5, \\ (-2 + 2s)\bar{z} + s, & -0.5 \leq \bar{z} \leq 0, \end{cases}$$

$g_4(\bar{z}) = -4(1 - s)\bar{z}^2 - 4(1 - s)\bar{z} + s$ ,  $-1 \leq \bar{z} \leq 0$ , and

$$g_5(\bar{z}) = \begin{cases} s, & -1 \leq \bar{z} \leq -0.7, \\ 1, & -0.7 \leq \bar{z} \leq -0.3, \\ s, & -0.3 \leq \bar{z} \leq 0. \end{cases}$$

Here  $0 \leq s \leq 1$  is the parameter to determine the amount of heterogeneity degree, identified as  $g_i(\bar{z}) = 1, \forall i$  at  $s = 1$ . Thus, the parameters  $\kappa_M(z)$  and  $\kappa_H(z)$  vary within  $s\kappa_M^0 \leq \kappa_M(z) \leq \kappa_M^0$ ,  $s\kappa_H^0 \leq \kappa_H(z) \leq \kappa_H^0$ .

The calculations (the results of which are shown in Fig. 9–11) were carried out for parameters as follows,  $l = 1$  mm,  $d = 0.5$  mm,  $h = 0.05$  mm,  $P_x = 0.3$  eV,  $E = 10^{-4}$  eV. Figs. 9 and 10 demonstrate that the inhomogeneities of both the magnetostatic field and  $H_0$  the saturation magnetization  $M_0$  give a significant shift of the eigenfrequencies real and imaginary parts. The functional type of the magnetic inhomogeneity is also matter (see Fig. 11).

Finally, it should be noted that the shift of the magnetostatic field's maximum to the middle of the ferromagnetic layer leads to shifting the maximum of the field from the layer's geometric boundary toward the line where  $\kappa_H(z)$  reaches its maximum value (see Fig. 11). This shift of the field maximum is the larger, the greater the degree of inhomogeneity of the  $\kappa_H(z)$ .

## Conclusions

An analytical regularization procedure has been developed for the dual series equations which appear in the problems of a vast class relating to diffraction of monochromatic plane waves by strip gratings placed at the boundary of a gyromagnetic medium. The problems concerning natural oscillations and their respective eigenfrequencies have been investigated for composite structures consisting of a lossy ferromagnetic layer that is inhomogeneous along one of the coordinates, and a perfectly conducting strip grating at one boundary of the ferromagnet, plus a graphene monolayer at the other, both placed in a magnetostatic field. It is shown that the structure proposed is an open resonant system supporting a set of complex eigenfrequencies with accumulation endpoints  $\sqrt{f_H^2 + f_H f_M}$  and  $f_H + 0.5f_M$ .

Here  $f_H$  and  $f_M$  are the characteristic frequencies of the ferromagnetic layer whose real parts lie in the range  $\sqrt{f_H^2 + f_H f_M} \leq \text{Re}(f) \leq f_H + 0.5f_M$ , while the imaginary parts are negative, such that the correspondent eigenoscillations demonstrate an exponential attenuation with time. Also, studied have been the effects which are exerted upon the eigenfrequencies and the natural oscillations by variations in geometric parameters of the structure and in characteristics of the graphene (in particular, the chemical potential and the relaxation energy of electrons), as well as by nonuniformity of the magnetostatic field and inhomogeneity of the saturated magnetization level of the ferromagnet. The results obtained can be useful for designing the microwave-range elements and devices.

## REFERENCES

- Jia, H., Yasumoto, K., and Toyama, H., 2005. Reflection and transmission properties of layered periodic arrays of circular cylinders embedded in magnetized ferrite slab. *IEEE Trans. Antennas Propag.*, **53**(3), pp. 1145–1153. DOI: 10.1109/TAP.2004.842654
- Monir, A., Sanada, A., Kubo, H., and Awai, I., 2003. Application of the 2-d finite difference-frequency domain method for the analysis of the dispersion characteristics of ferrite devices. In: *Proc. 33rd European Microwave Conference*. Munich, Germany, 2–10 Oct. 2003. Munich: IEEE, pp. 1175–1177.
- Brovenko, A., Melezhik, P., and Poyedinchuk, A., 2012. Resonance scattering of a plane electromagnetic wave by a ferrite-stripe grating-metamaterial structure. *Telecommunications and Radio Engineering*, **71**(12), pp. 1057–1074. DOI: 10.1615/TelecomRadEng.v71.i12.10
- Brovenko, A.V., Melezhik, P.N., Poyedinchuk, A.E., and Troshchilo, A.S., 2020. Diffraction of electromagnetic waves on the composite structure "strip grating – ferromagnetic half-space": resonances on surface waves. *Radiophys. Elektron.*, **25**(1), pp. 11–20 (in Russian). DOI: <https://doi.org/10.15407/rej2020.01.011>
- Masalov, S.A., Ryzhak, A.V., Sukharevsky, O.I., and Shkil, V.M., 1999. *Physical Foundations of Range Technologies "Stealth"*. St. Petersburg, Russia: Mozhaisky VIKU Publ. (in Russian).
- Brovenko, A., Vinogradova, E., Melezhik, P., Poyedinchuk, A., and Troshchilo, A., 2010. Resonance wave Scattering by strip grating adjusted to ferromagnetic medium. *Prog. Electromagn. Res. B*, **23**, pp. 109–129. DOI: 10.2528/PIERB10012203
- Brovenko, A.V., Melezhik, P.N., Poyedinchuk, A.Y., and Yashina, N. P., 2006. Surface resonances of metal stripe grating on the plane boundary of metamaterial. *Prog. Electromagn. Res.*, **63**, pp. 209–222. DOI: 10.2528/PIER06052401
- Lim, J., Bang, W., Trossman, J., Amanov, D., and Ketterson, J., 2018. Forward volume and surface magnetostatic modes in an yttrium iron garnet film for out-of-plane magnetic fields: Theory and experiment. *AIP Advances*, **8**(5), 056018 DOI: 10.1063/1.5007263
- Damon, R.W., and Eshbach, J.R., 1961. Magnetostatic modes on a ferromagnetic slab. *J. Phys. Chem. Solids*, **19**(3–4), pp. 308–320. DOI: 10.1016/0022-3697(61)90041-5
- Gurevich, A.G., and Melkov, G.A., 1994. *Magnetic Oscillations and Waves*. Moscow: Fizmatgiz (in Russian).
- Novoselov, K.S., Geim, A.K., Morozov, S.V., Jiang, D., Dubonos, S.V., Zhang, Y., Grigorieva, I.V., and Firsov, A.A., 2004. Electric field effect in atomically thin carbon films. *Science*, **306**(5696), pp. 666–669. DOI: 10.1126/science.1102896
- Nair, R.R., Blake, P., Grigorenko, A.N., Novoselov, K.S., Booth, T.J., Stauber, T., Peres, N.M.R., and Geim, A.K., 2008. Fine structure constant defines transparency of graphene. *Science*, **320**, pp. 1308–1308. DOI: 10.1126/science.1156965
- Novoselov, K.S., Geim, A.K., Morozov, S.V., Jiang, D., Katsnelson, M.I., Grigorieva, I.V., Dubonos, S.V., and Firsov, A.A., 20025. Two-dimensional gas of massless Dirac fermions in graphene. *Nature*, **438**, pp. 197–200. DOI: 10.1038/nature04233
- Kaipa, C.S.R., Yakovlev, A.B., Hanson, G.W., Padooru, Y.R., and Medina, F., 2012. Mesa enhanced transmission with a graphene-dielectric microstructure at low-terahertz frequencies. *Phys. Rev. B*, **85**, 245407. DOI: 10.1103/PhysRevB.85.245407
- Padooru, Y.R., Yakovlev, A.B., Kaipa, C.S.R., Hanson, G.W., Medina, F., and Mesa, F., 2013. Dual capacitive-inductive nature of periodic graphene patches: Transmission characteristics at low-terahertz frequencies. *Phys. Rev. B*, **87**, 115401. DOI: 10.1103/PhysRevB.87.115401
- Brovenko, A., Melezhik, P., Poyedinchuk, A., Yashina, N., and Granet, G., 2009. Resonant scattering of electromagnetic wave by stripe grating backed with a layer of metamaterial. *Prog. Electromagn. Res. B*, **15**, p. 423–441. DOI: 10.2528/PIERB09052302

17. Hanson, G.W., 2008. Dyadic Green's functions and guided surface waves for a surface conductivity model of grapheme. *J. Appl. Phys.*, **103**(6), 064302. DOI: 10.1063/1.2891452
18. Brovenko, A.V., Melezhik, P.N., Panin, S.B., and Poyedinchuk A.Ye., 2013. Numerical-analytical method for solving problems of the waves diffraction on layered-inhomogeneous medium. *Physical Fundamentals of Instrumentation*, **2**(1), pp. 34–47 (in Russian).
19. Brovenko, A., Melezhik, P., Panin, S., and Poyedinchuk, A., 2013. Wave diffraction on a stripe grating at a boundary of a layered inhomogeneous medium: method of analytic regularization. *Radiophysics and Quantum Electronics*, **56**, pp. 238–248. DOI: 10.1007/s11141-013-9429-x
20. Shestopalov, V.P., and Sirenko, Yu.K., 1989. *Dynamical lattice theory*. Kiev: Naukova Dumka Publ. (in Russian).
21. Chandezon, J., Granet, G., Melezhik, P.N., Poyedinchuk, A.Ye., Sirenko (ed.), Yu.K., Sjoberg, D., Strom, S. (ed.), Tuchkin, Yu.A., and Yashina, N.P., 2010. *Modern theory of grating. Resonant scattering: analysis techniques and phenomena*. New York, Springer Sciens+Business Media, LCC.
22. Shestopalov, V.P., Tuchkin, Yu.A., Poyedinchuk, A.Ye., and Sirenko, Yu.K., 1997. *New methods for solving direct and inverse problems of diffraction theory. Analytical regularization of boundary value problems of electrodynamics*. Kharkov: Osnova Publ. (in Russian).
23. Stancil, D.D., 1980. Magnetostatic waves in nonuniform bias fields including exchange effects. *IEEE Trans. Magn.*, **16**(5), pp. 1153–1155.
24. Wilts, C.H., and Prasad, S., 1981. Determination of magnetic profiles in implanted. Garnets using ferromagnetic resonance. *IEEE Trans. Magn.*, **17**(5), pp. 2405–2414.

Received 24.02.24

А.В. Бровенко, П.М. Мележик,  
А.Ю. Поєдинчук, О.Б. Сенкевич, Н.П. Яшина

Інститут радіофізики та електроніки ім. О.Я. Усикова НАН України  
вул. Акад. Проскури, 12, м. Харків, 61085, Україна

#### ВЛАСНІ ЕЛЕКТРОМАГНІТНІ КОЛИВАННЯ ВІДКРИТОЇ КОМПОЗИТНОЇ СТРУКТУРИ, ЩО МІСТИТЬ ЕЛЕКТРОПРОВІДНУ СТРІЧКОВУ ГРАТКУ, НЕОДНОРІДНИЙ ФЕРИТОВИЙ ШАР І ГРАФЕНОВИЙ МОНОШАР

**Предмет і мета роботи.** Розглянуто задачу про власні коливання та відповідні власні частоти композитної структури, що є неоднорідною вздовж однієї з координат і складається з феромагнітного шару з втратами, котрий знаходиться у магнітостатичному полі. На одній з граничних поверхонь розміщено ідеально провідну стрічкову ґратку, а на іншій — графеновий моношар.

**Методи та методологія.** Для розв'язання задачі розроблено метод аналітичної регуляризації парних суматорних рівнянь, до яких зводиться широкий клас задач дифракції. Зокрема, це стосується задач про дифракцію монохроматичних плоских хвиль на стрічкових ґратках, що розташовані на межі гіромагнітного середовища. Для обчислення амплітуд власних електромагнітних полів використано однорідну систему лінійних алгебричних рівнянь, розв'язок якої розшукується методом редукції. Корені детермінанта цієї системи є комплексними власними частотами досліджуваної структури. Матеріальні параметри, котрі було прийнято в розрахунках для феромагнітного шару, відповідають даним залізо-ітрієвого гранату.

**Результати.** Розроблено пакети програм, за допомогою яких чисельно проаналізовано залежності власних полів і комплексних власних частот від геометричних параметрів структури (ширини щілин ґратки, її періоду та товщини феромагнітного шару), а також від електродинамічних параметрів феромагнетика та параметрів графену (хімічного потенціалу та енергії релаксації електронів). Установлено низку закономірностей у динаміці цих залежностей. Також оцінено вплив неоднорідності параметрів феритового шару на власні частоти та власні польові функції структури.

**Висновки.** Показано, що досліджувана структура є відкритою коливальною системою з набором комплекснозначних власних частот із кінцевими точками накопичення. Дійсні частини цих власних частот лежать у певному інтервалі, який визначається характерними частотами феритового шару; уявні частини є негативними, тобто відповідні цим частотам власні коливання згасають експоненціально в часі. Ребра ґраток є «дзеркалами», від яких відбиваються поверхневі власні коливання, а феромагнітне середовище ці коливання підтримує. Отримані результати можуть бути використані при створенні елементної бази і пристроїв НВЧ-діапазону.

**Ключові слова:** феритовий шар, графен, стрічкова ґратка, аналітичний метод регуляризації, власні коливання, власні частоти.